

Role of network geometry on fluid displacement in microfluidic color-changing windows

Ahmet Burak Uçar¹, Orlin D. Velev^{**1} and Hyung-Jun Koo^{*2}

¹Department of Chemical and Biomolecular Engineering, North Carolina State University, Raleigh, NC 27695, USA

²Department of Chemical and Biomolecular Engineering, Seoul National University of Science and Technology, Seoul, Republic of Korea

(Received December 30, 2015, Revised July 5, 2016, Accepted July 8, 2016)

Abstract. We have previously demonstrated a microfluidic elastomer, which changes apparent color and could have potential applications in smart windows. The practical use of such functional microfluidic systems requires rapid and uniform fluid displacement throughout the channel network with minimal amount of liquid supply. The goal of this simulation study is to design various microfluidic networks for similar applications including, but not limited to, the color-switching windows and compare the liquid displacement speed and efficiency of the designs. We numerically simulate and analyze the liquid displacement in the microfluidic networks with serpentine, parallel and lattice channel configurations, as well as their modified versions with wide or tapered distributor and collector channels. The data are analyzed on the basis of numerical criteria defined to evaluate the performance of the corresponding functional systems. We found that the lattice channel network geometry with the tapered distributors and collectors provides most rapid and uniform fluid displacement with minimum liquid waste. The simulation results could give an important guideline for efficient liquid supply/displacement in emerging functional systems with embedded microfluidic networks.

Keywords: COMSOL simulation; microfluidic network; flow uniformity; liquid displacement efficiency; color-changing smart windows

1. Introduction

Microfluidics is widely used in lab on a chip devices due to its ease of design and implementation, low fabrication cost, and small fluid volume needs. The laminar nature of the flow enables these devices to provide suitable conditions for processes such as particle sorting, biological synthesis and analysis (Stone and Stroock 2004, Mark, Haerberle *et al.* 2010, Gunther and Jensen 2006). Going beyond devices, microfluidic composites with embedded micro-channel networks are an emerging class of functional soft materials (Koo and Velev 2013, Olugebefola, Aragon *et al.* 2010). Self-healing surfaces (Toohey, Fan *et al.* 2007, Murphy and Wudl 2010, Hager, Greil *et al.* 2010), tunable fluidic antennas (So, Thelen *et al.* 2009), photocurable shape

*Corresponding author, Professor, E-mail: hjkoo@seoultech.ac.kr

** Corresponding author, Professor, E-mail: odvelev@ncsu.edu

memory materials (Chang, Uçar *et al.* 2009), color changing elastomers (Uçar and Velev 2012, Morin, Shepherd *et al.* 2012), and re-generable photovoltaic devices (Koo and Velev 2013a) are just a few examples of such applications. Rapid and uniform supply and displacement of fluids in a given channel network is essential for more efficient operation of such functional fluidic materials.

The role of the channel geometry on the fluid flow characteristics (e.g., displacement rate, flow uniformity, etc.) in the networks has been investigated in many theoretical, numerical, and experimental studies to find a channel design for rapid liquid displacement (Olugebefola, Aragon *et al.* 2010, Saias, Autebert *et al.* 2011, Liu, Li *et al.* 2010, Cho and Kim 2010, Wang *et al.* 2002, Wang 2011). These studies have focused on various fluidic systems with heat exchange or ‘irrigation’ functionality. Based on the constructal law, it was found that tree-like structures provide high rate of liquid delivery from one point to another one (i.e., they have good hydraulic conductance) (Bejan and Lorente 2006, Reis 2006, Domachuk, Tsioris *et al.* 2010, Wu, Hansen *et al.* 2009).

The functional goal of certain microfluidic materials involves ‘healing’ a surface crack inspired by a human skin, or having simultaneous reactions or displacing liquid in a channel network in a controlled fashion (Toohey, Sottos *et al.* 2007, Murphy and Wudl 2010, Hager, Greil *et al.* 2010, Uçar and Velev 2012, Morin, Shepherd *et al.* 2012). Beside the rapid displacement, such functional microfluidic materials require a uniform delivery of the liquid over the whole surface area (Cho and Kim 2010, Tondeur, Fan *et al.* 2011a, b, c, Wang, Lorente *et al.* 2007, Commenge, Saber *et al.* 2011). The classic parallel channel networks are used in many micro-channel designs; however, the simple implementation of the parallel networks could lead to mal-distribution of the transported fluids (Liu, Li *et al.* 2010, Solovitz and Mainka 2011, Lee, Lorente *et al.* 2009).

We earlier reported a class of color changing microfluidic elastomers (Uçar and Velev 2012), which are operating on the basis of a network of channels filled with liquids whose refractive index is matched to the matrix material. By injecting dye solutions into the channel networks and consecutively replacing the medium, the apparent color of the microfluidic material and its light transmittance can be controlled in the visible and near-infrared regions. Other prototypes of channel network-based smart windows for control of other physical properties, such as luminescence and surface temperature, have also been recently reported (Morin, Haeberle *et al.* 2012, Hatton, Wheeldon *et al.* 2013). We present here the results of an extensive simulation study on fluidic transport in various 2-D channel network geometries, in the effort of achieving rapid and uniform displacement of the operational liquid phase in the functional microfluidic materials. The simulation results allow evaluation of delivery speed, flow uniformity and liquid use efficiency in the microfluidic networks. First, the classic parallel channel networks (H-networks) are compared to the serpentine networks (S-networks) used in the color changing elastomers we reported earlier (Uçar and Velev 2012). Then, to optimize the channel geometry, the effect of the H-network modification on liquid displacement performance is evaluated by widening or tapering the distributor and collector channels. Finally, liquid displacement in the lattice-type networks – the modified H-networks with additional interconnecting vertical channels – is investigated and compared to that in the S- and H-networks.

2. Channel network design and simulation

The objective of this simulation work is to identify which channel geometry in a functional

microfluidic material allows the most rapid and uniform liquid displacement while minimizing waste, which typically occurs due to non-uniform liquid displacement. The initial designs for the simulation study are the S-network with a serpentine channel (Fig. 1(c)), used in our previous experimental work (Figs. 1(a) and 1(b)) (Uçar and Velev 2012), and the H-network with symmetrical distributor and collector channels (D/Cs) connecting the horizontal, parallel channels (Fig. 1(d)). The H-networks are widely used in devices requiring parallel flows. The uniformity of the H-networks could be improved by modifying channel geometry of the D/Cs. The H-networks with wide or tapered D/Cs were designed and compared to the H-networks with normal D/Cs. Lattice networks, which are essentially H-networks with interconnecting vertical channels, were also tested and compared with the S- and the H-networks.

We used COMSOL multiphysics software package (ver. 4.2a) for the fluid flow simulation study. The transport of liquid injected into the microfluidic networks was simulated by using the equations of “Laminar Flow” and “Transport of Diluted Species”, predefined in COMSOL as follows

$$\rho \vec{v} \cdot \nabla \vec{v} = \nabla \cdot \left\{ -\vec{p} + \eta (\nabla \vec{v} + (\nabla \vec{v})^T) \right\} \quad (\text{“Laminar Flow” equation})$$

$$\frac{\delta c}{\delta t} = -\vec{v} \cdot \nabla c + D \nabla \cdot \nabla c \quad (\text{“Transport of Diluted Species” equation})$$

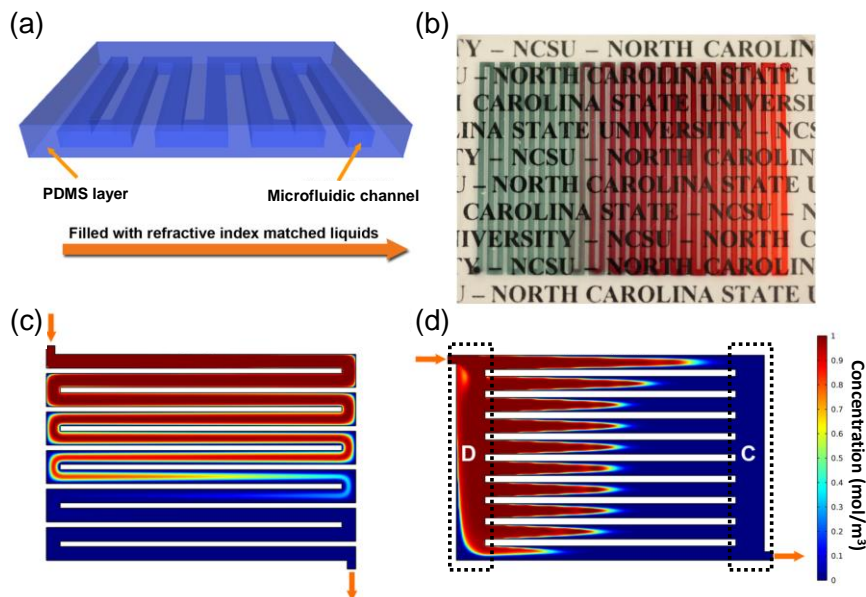


Fig. 1 (a) Schematics of the single-layered color changing elastomers containing the serpentine channel network with pressure-driven displacement ($\Delta P \approx 20\text{--}80$ kPa). The liquid in the channels can be replaced with clear or colored, refractive index matched solutions to control the transmittance spectra of the material. (b) Photographic image of an actual prototype of the microfluidic color changing material with the serpentine channels embedded in polydimethylsiloxane (PDMS) rubber (Uçar and Velev 2012). (c-d) Simulation results of typical flow patterns during liquid replacement (c) in the S-network design and (d) in the H-network design. The blue-to-red color scale represents the concentration of a solute from the displacing liquid. ‘D’ and ‘C’ in (d) indicate the distributor and the collector channels, respectively

where ρ , η and \vec{v} are the density, viscosity and velocity of the injected solution, respectively. c is the concentration of the solution and D is the diffusion coefficient of the solute in the solution. First, the velocity and pressure profiles of the flow at steady state were calculated by the Laminar Flow equation set with boundary conditions of constant inlet and outlet pressure difference (i.e., pressure drop, $\Delta P = 1$ or 30 kPa). The resulting velocity values of the liquid flowing in the channel were incorporated into the Transport of Diluted Species equation with constant inlet concentration of a solute (1 mol m^{-3}). This equation takes into account both diffusion and convection effect for the solute transport in the flow. The velocity values, \vec{v} , obtained from the Laminar Flow equation are needed to calculate the convection-driven solute transport. The flow in channels with solid walls was modeled and the properties of the PDMS matrix were not incorporated in the analysis. All parameters and constraints for the simulation were selected to be as close to the experimental ones (Uçar and Velev 2012) as possible. The physical properties, e.g., density and viscosity, of 61% Glycerol – Water mixture (with refractive index matched to PDMS) were used for the liquid parameters in the simulation. The main constraints in all simulations were the fixed total matrix area (860 mm^2) and the channel area (75% of the matrix area) whereas the channel sizes (and thus void sizes) varied. The cross-sectional area of the inlet and outlet channels, and pressure drop ($\Delta P = 1$ kPa, unless otherwise stated) in the system were kept constant so that all networks would potentially require the same pumping power. More details about the parameters and constraints for the simulation can be found in section A of Supplementary Information.

Initially, we tested the S- and H-networks with the different channel widths varying from 0.35 mm to 0.95 mm, to evaluate the effect of channel size on the displacement efficiency. After this test, we performed the simulation within the target channel size range (~ 300 - $350 \mu\text{m}$). Our models in this simulation study were designed and tested as 2-D. Due to thin, but long channels with rectangular cross-section in the network, we incorporated the effect of the depth of the channels by using the “shallow channel approximation” mode in COMSOL. This mode adds an additional term for a drag force generated by the top and the bottom channel walls into the Laminar Flow equation. This approximation is useful to improve the results of simple 2D models as they exclude the boundaries that have significant effect on the flow, and shallow channel approximation takes the effects of these boundaries into account.

We limited the scope of our analysis to two major criteria relevant to smart microfluidic windows: Most rapid overall liquid displacement and least liquid waste during the displacement. These criteria are needed to achieve cost effective and visually smooth color change in the windows based on microfluidic elastomer composites. The degree of the liquid displacement at a given time was obtained from the average solute concentration in a channel network. The average concentration in a network could increase up to the concentration for the inlet boundary condition, 1 mol m^{-3} , which we defined as 100% liquid displacement. For instance, when the average concentration of the liquid in a whole network is 0.3 mol m^{-3} at a given time, the liquid displacement is 30%. The average concentration of the liquid at a given time in the channel networks was directly obtained from processing COMSOL output data. The liquid use efficiency and the liquid waste rate were calculated using the following formulas

$$\eta_{LiqUse} = \frac{C_{Surface}}{J_{Inlet} \times t} \quad (1)$$

$$\alpha = 100 \times (1 - \eta_{LiqUse}) \quad (2)$$

where η_{LiqUse} is the dimensionless liquid use efficiency, $C_{Surface}$ is the surface concentration of the liquid in the channel network in mol m^{-1} , J_{Inlet} is the total flux magnitude at inlet in $\text{mol m}^{-1} \text{s}^{-1}$, t is the time in s, and α is the liquid waste rate in %. The surface concentration (mol m^{-1}), equivalent to the total channel area times the average concentration, was also obtained from COMSOL.

The goal in this study is to achieve a network design which enables displacing at least 90% of the original liquid in the network within 10 s with a waste rate of <10%, so that the whole area of the material could exhibit a rapid and an efficient color changing performance. Also for practical purposes (ease of fabrication, shape of typical windows, potential installations on symmetrical surfaces, etc.), we aim to avoid significant deviation from the overall rectangular shape of the network.

3. Simulation results and analysis

3.1 Comparison of liquid displacement in S- and H-networks

We compared S- and H-networks with different widths and thus different numbers of channels due to the constraint of the fixed total network area. Each network structure was named by its network shape (S- or H-) and the number of the horizontal channels in the main network. For example, S-19 represents the S-network consisting of 19 horizontal channels. First, the simulated liquid displacement in the S-19 (Fig. 2(a)) and the H-19 (Fig. 2(b)) networks with equal inlet pressure of 1 kPa is compared. (Since we use “inlet pressure” as the relative value to outlet pressure in this study, it is equivalent to pressure drop between inlet and out.) More than 50% of the liquid in the H-19 network is replaced in 10 s, whereas the liquid displacement percentage in the S-19 network does not even reach to 5% for the same time period. To achieve ~50% of liquid displacement after 10 s of liquid supply, the S-19 requires an inlet pressure more than 30 kPa as shown in Fig. 2(c). The time-dependent average concentrations in the S- and the H-networks with 19 and 51 channels are plotted in Fig. 2(d) (more plots are provided in Fig. S1 of Supplementary Information, where the time-dependent average concentrations in the S- and H-networks with 19, 25, 37, and 51 channels are compared). The slope of the plots represents the liquid displacement rate in each network. The difference in the displacement rates between H- and S-networks under the same inlet pressure is apparent. For instance, after the liquid supply for 20 s at 1 kPa inlet pressure, ~32% of the original liquid in the H-51 network was replaced by the displacing liquid, whereas only ~0.3% displacement was achieved in the S-51 network, i.e., H-51 network had ~100 times larger liquid displacement speed. Thus, the H-networks enable more rapid liquid displacement than the S-networks.

The rates of liquid waste in the S- and the H-networks were qualitatively compared based on the onset time of the liquid loss. The H-networks start to drain the supplied liquid before they could replace 50% of the liquid in the network (as seen in Fig. 2(b)), whereas no liquid waste was observed in S-networks until ~90% of the liquid displacement (data not shown). As the liquid in the S-network flows along a single path, the S-networks outperform the H-networks in terms of efficient liquid displacement with minimal liquid waste.

Even though the S-networks have a benefit in terms of liquid use efficiency, however, we decided to modify the geometry of the H-networks further, as they offered significantly more rapid liquid displacement and lower injection pressure than the S-networks (e.g., Fig. 2(b) vs. Fig. 2(a) and (c)). Lowering the inlet pressure is important in a practical sense because the inlet pressure is

proportional to the energy required for injecting the displacing liquid. The major disadvantage of the H-networks is the flow mal-distribution similarly to the cases reported earlier for other systems (Cho and Kim 2010, Lee, Lorente *et al.* 2009).

The distribution uniformity of solution injected into the H-network is affected by the channel width. Fig. 3 illustrates the liquid displacement in the H-networks with different channel numbers (H-19, 25, 37, and 51) at the moment of 30% liquid displacement under the same inlet pressure of 1 kPa. As the channel number increases and therefore the channel width decreases, the required time for 30% liquid displacement increases. Interestingly, the H-networks with fewer numbers of the horizontal channels, i.e., with the wider channels, achieve more uniform as well as faster liquid displacement than the ones with narrower channels. The H-networks with narrower channels like H-51 have more no-slip boundaries between the flow and the channel wall, thereby resulting in the slower liquid displacement. In the H-networks with more channels, the flow pattern becomes more “inverse-parabolic”, causing less uniform flow distribution.

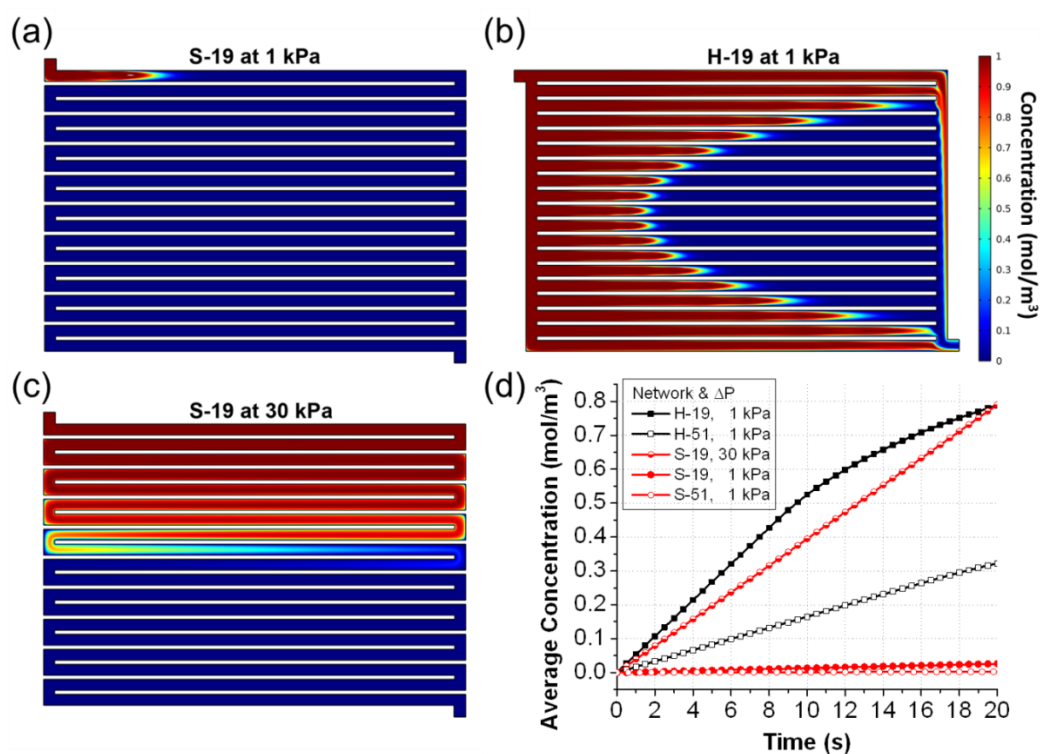


Fig. 2 (a-c) Simulation results of the liquid displacement in the S- and the H-networks at 10 s. (a) S-19 with 1 kPa inlet pressure. (b) H-19 with 1 kPa inlet pressure. (c) S-19 with 30 kPa inlet pressure. The number next to the network type (S- or H-) shows the number of channels in the main network. (d) Average concentrations of the dye solution in the whole networks are plotted for the S- and the H-networks with different channel numbers under 1 kPa and 30 kPa inlet pressures (full list of the plots is shown in Fig. S1 of Supplementary Information). Under the same inlet pressure, the H-networks are superior to the S-networks in terms of the liquid displacement speed

The non-uniform flow in the H-networks with narrower channels also leads to the negative consequence of increased liquid waste. We compared the liquid waste rates of the networks shown in Fig. 3 at the time of the 30% liquid displacement. The liquid waste rate of the H-19 network (Fig. 3(a)) was still negligible (0.0%), whereas the corresponding value for H-51 network (Fig. 3(d)) was $\sim 3.3\%$. We found that the H-networks with wider channels are superior to those with narrower channels in terms of flow uniformity, rapid displacement rate and low liquid waste. However, since the minimum channel size distinguishable by human eyes from a 1 m distance is $\sim 350 \mu\text{m}$ (Russ 2011), channel dimensions not larger than this size would be more preferable for the target application of smart windows. Our challenge in the following simulations is to optimize the H-51 network with $350 \mu\text{m}$ maximal horizontal size of the channels.

3.2 Geometry effect of distributor and collector channels (D/Cs) on liquid displacement performance in H-networks

One of the means to improve flow uniformity in the H-networks would be using channels with individually different sizes, i.e., multiple-scale designs. For instance, tuning all the individual channel sizes in the whole network could enable equating all flow resistances throughout the network. However, to comply with our channel size restriction and preserve the visual symmetry and uniformity of the channel network, we introduced only one more scale to the system by having the D/C channels with different size. D/Cs with either simply wider (Cho and Kim 2010, Tondeur, Fan *et al.* 2011a, b, c, Lee, Lorente *et al.* 2009) or tapered (Commonge, Saber *et al.* 2011, Solovitz and Mainka 2011) geometries lead to smaller differences in flow resistance between the channels.

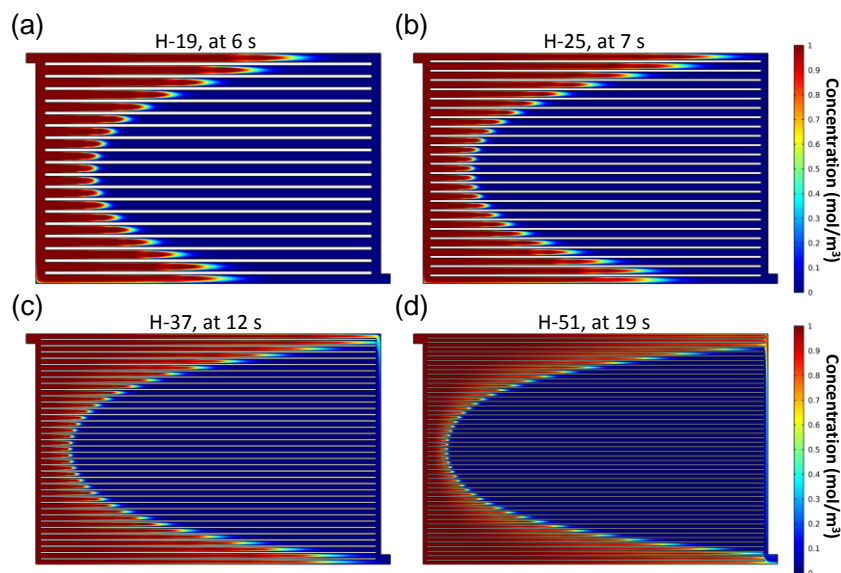


Fig. 3 Simulation results of liquid displacement in H-networks with different channel sizes at $\sim 30\%$ liquid displacement (i.e., when the average concentration in each channel network reaches $\sim 0.3 \text{ mol m}^{-3}$). (a) H-19 network at 6 s (horizontal channel width = $930 \mu\text{m}$). (b) H-25 network at 7 s (horizontal channel width = $710 \mu\text{m}$). (c) H-37 network at 12 s (horizontal width = $480 \mu\text{m}$). (d) H-51 network at 19 s (horizontal width = $350 \mu\text{m}$). The images also visually illustrate the flow non-uniformity in each network

To investigate the effect of such designs, we compared the liquid displacement performance of the H-networks with the wide or tapered D/Cs (Fig. 4). In all these comparisons, we used H-51 networks while we varied the D/C size and shape. The tapering ratio given in the figures is the ratio of long edge width of the D/Cs to the short edge width, which are normalized by the horizontal channels width ($\sim 350 \mu\text{m}$). We tested several ratios from 1:1 to 11:1 (Fig. 4), where 1:1 ratio means the single-scale network of Fig. 3(d).

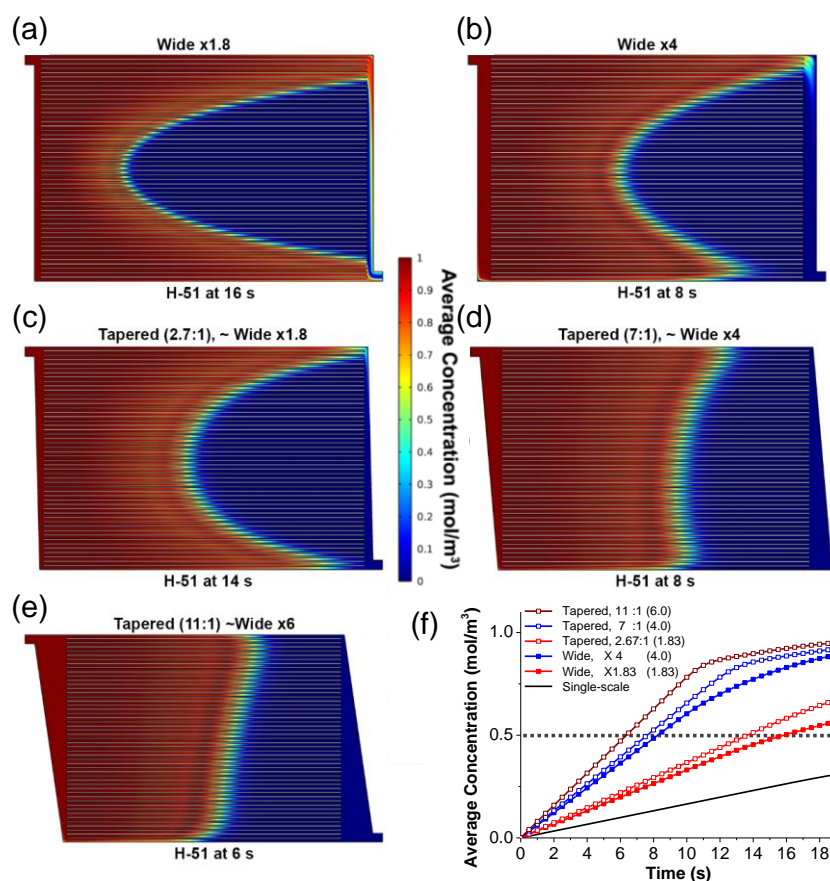


Fig. 4 Simulation results of liquid displacement in the multiple-scale H-networks with the ‘wide’ (a,b) or ‘tapered’ (c-e) D/Cs at 50% liquid displacement; (a) D/Cs 1.8 times wider than the main channel, (b) D/Cs 4 times wider than the main channel size, (c) tapered D/Cs with the 2.7:1 ratio, (d) tapered D/Cs with the 7:1 ratio, (e) tapered D/Cs with the 11:1 ratio. Due to the fixed network area constraint, the main horizontal channel width is slightly varied in $\sim 350 \mu\text{m}$ depending on the D/C geometries. The average widths of the tapered D/Cs in (c) and (d) are equal to those of the wide, non-tapered D/Cs in (a) and (b), respectively. (f) Time-dependent average concentration in the H-51 networks with the wide or the tapered D/Cs (a larger data set is shown in Fig. S2 of Supplementary Information along with further comparison of the wide and the tapered D/Cs). The numbers in the parentheses are the average D/C widths normalized by the main horizontal channel width. The dotted grey line indicates the 50% liquid displacement. Having the wide D/Cs reduces flow resistance of the network. Tapering the D/Cs improves the flow uniformity more significantly than simply using wide D/Cs, although it creates a slight deformation of rectangular shape of the network

The snapshots in Figs. 4(a)–4(e) visualize the liquid distribution in the channel networks with the wide or tapered D/Cs at the same liquid displacement of 50% and Fig. 4(f) shows the time-dependent liquid displacement in each network. Compared to the single-scale networks, the use of wider D/Cs not only improves the flow uniformity but also increases the displacement rate (compare Figs. 4(a) and 4(b) to Fig. 3(d)). For instance, the single-scale H-51 network in Fig. 3(d) replaces 30% of the liquid in 19 s, whereas for the H-51 network with 4 times wider D/Cs in Fig. 4(b), it takes only 8 s to replace 50% of the liquid in the network. To investigate the effect of the tapered D/Cs on the liquid displacement, two H-networks with the tapered D/Cs with different tapering ratios, 2.67:1 and 7:1, were designed (Figs. 4(c) and (d)). The tapered D/Cs in Fig. 4(c) and (d) have the equal average width with the non-tapered, wide D/Cs in Figs. 4(a) and 4(b), respectively. At the same 50% liquid displacement, the apparent flow patterns in the networks with the tapered D/Cs are more uniform than those in the networks with the non-tapered D/Cs (Fig. 4(a) vs. Fig. 4(c) and Fig. 4(b) vs. Fig. 4(d)). The networks with the tapered D/Cs also displace the liquid in the network more rapidly. For example, it takes 7.7 s for the H-51 network with the 7:1 tapered D/Cs to reach the 50% liquid displacement (Fig. 4(d)), whereas the network with the evenly wide D/Cs in Fig. 4(b) requires longer time (8.3 s) for the same liquid displacement. Thus, the tapered D/Cs improve the H-networks in both aspects of uniform and rapid liquid replacement. Further comparison of the H-networks with the tapered and the wide D/Cs is discussed in section C of Supplementary Information.

Solovitz and Mainka (2011) reported that for a uniform flow distribution in channel networks with a constant aspect ratio, the D/Cs should taper with the ratio of $k^{0.25}$, where k stands for the number of the channels in the network. For the H-51 network, the first tapering ratio of 2.7:1 in Fig. 4(c) was estimated via this power law ($51^{0.25} \cong 2.7$). However, it turns out that as the tapering ratio increases to 7:1 (Fig. 4(d)) and 11:1 (Fig. 4(e)), we could obtain more uniform and rapid liquid displacement (8 s for 7:1 tapering ratio and 6 s for 11:1 tapering ratio at the 50% liquid displacement). This may be because we did not taper the whole cross-sectional area (depth remained constant in our simulation) unlike the Solovitz and Mainka's work. Even though larger tapering ratio could be more effective for uniform and rapid liquid displacement, this could noticeably change the original rectangular shape of the network and complicate its fabrication. In another study to achieve uniform residence time distribution in a microreactor (Renault, Colin *et al.* 2012), the optimal tapering degree for the parallel networks has been expressed in terms of angle, which is around 10° for the H-51 network. This would correspond to a tapering ratio of 13~14:1 in our system. This high tapering ratio could also significantly deform the original rectangular shape of the network, which is undesirable for smart windows, while being of little consequence for compact devices such as fuel cells (Tondeur, Fan *et al.* 2011a, b, c).

The plot in Fig. 5 compares the required time for the 90% liquid displacement and the liquid use efficiencies of the H-51 networks with wide vs. tapered D/Cs. With the constant average D/C width of 4 (7:1 tapered, 5.5:2.5 wide/tapered and 4× wide), the networks with higher tapering ratio allow more rapid liquid displacement with less liquid waste. For example, compared to the network with only wide D/Cs (4× wide), the tapered network with 7:1 ratio reaches 90% liquid displacement in ~3 s shorter time with 5% less liquid waste rate. The best performing network among the tested channel networks is the one with the tapered D/Cs with the highest ratio, 11:1 (with average thickness of 6), which displaces 90% of the liquid in ~15 s with the lowest liquid loss rate (~21%). However, this liquid loss rate is still above our target rate of 10%. In summary, the networks with the tapered D/Cs with a high tapering ratio produce satisfactory performance in terms of the liquid displacement speed, while their liquid use efficiencies still need to be improved.

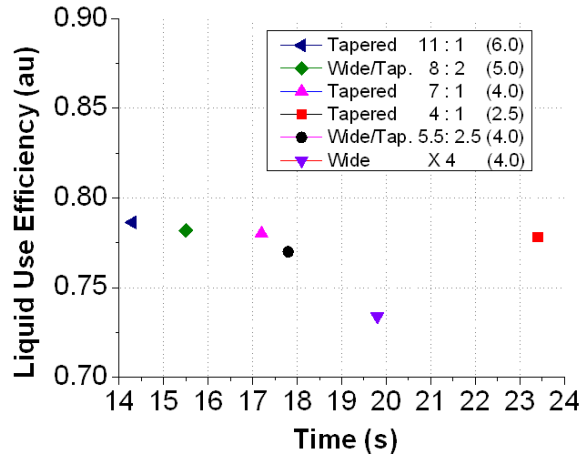


Fig. 5 Comparison of the liquid use efficiencies and the elapsed times of the H-51 networks with the wide or tapered D/Cs at 90% liquid displacement. The numbers in the parentheses are the average D/C widths normalized by the main horizontal channel width. The networks with only wide (non-tapered) D/Cs waste more liquid

3.3 Liquid displacement performance in lattice networks

We next evaluated the performance of the lattice-type channel networks, which are also a common geometry in fluidic networks, as they provide smaller pressure drops and more uniform flow distribution in the network (Tondeur, Fan *et al.* 2011a, b). The lattice network is essentially an H-network with interconnecting vertical channels. We constructed a lattice network consisting of 34 horizontal and 49 intersecting vertical channels, so that the main network channel size could be similar to the one used in the previously tested H-51 networks. Fig. 6(a) illustrates the simulated flow pattern during the liquid replacement in the lattice network with the tapered D/C (tapering ratio = 4:1). This lattice network achieves replacement of 90% of the liquid in ~13 s, which is almost twice faster than the time required in the corresponding H-network with the same tapering ratio (~23.5 s, see the red square point in Fig. 5). Figs. 6(b) and 6(c) compare the single-scale and the various multiple-scale lattice networks in terms of the time-dependent liquid displacement and the liquid use efficiency at the 90% liquid displacement. The single-scale lattice network replaces 90% of the liquid in less than 17 s with a liquid waste rate of less than 20% (see the orange square point in Fig. 6(c)). When the wide or the tapered D/Cs are incorporated in the lattice network, both the liquid displacement speed and the liquid use efficiency increase. Among the lattice networks with the various geometries we tested in Figs. 6(b) and 6(c), the lattice network with 4:1 tapered D/Cs, shown in Fig. 6(a), achieves the most rapid liquid displacement with 10% liquid waste rate, which is the target value of this study. Compared to the best H-network with 11:1 tapered D/Cs in Fig. 4(e), this lattice network enables not only a higher displacement rate (~13s < ~14.5s for 90% liquid displacement) but also much smaller liquid waste rate (~10% < 21%). These findings show that the presence of vertical channels improves the flow access of the network, thereby allowing more uniform and rapid liquid displacement. Furthermore, thanks to the low tapering ratio in the lattice network's geometry, no significant deviation from the overall rectangular shape is required

to achieve the target performance. Thus, this design has been identified as the best choice for further development of engineered networks for similar applications. Further modification could be done to improve network’s liquid displacement speed and efficiency, such as introducing more dimensions in the networks (see section D in Supplementary Information).

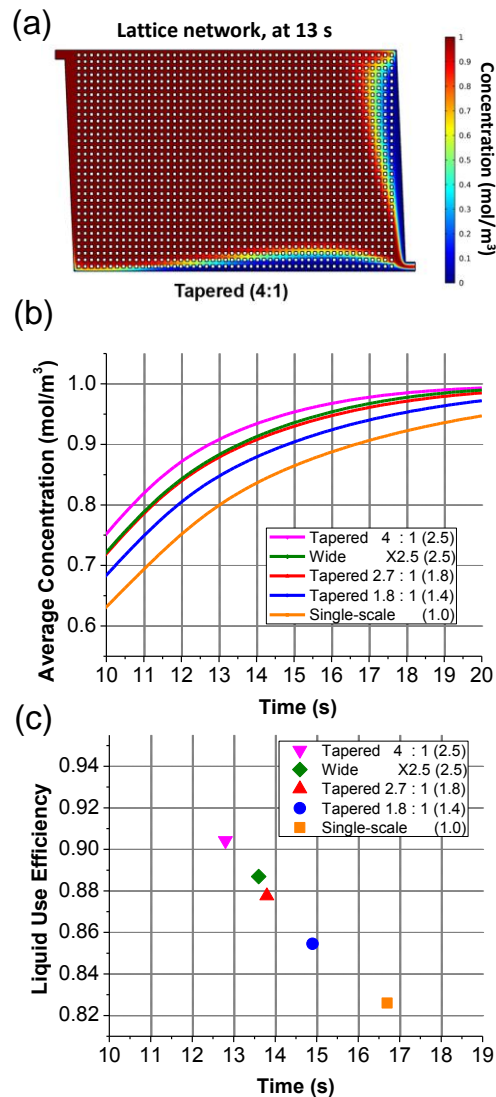


Fig. 6 Simulation results of the liquid displacement in the lattice networks with wide or tapered D/Cs. (a) Snapshot of liquid flow pattern in the lattice network with the 4:1 tapered D/Cs at the 90% liquid displacement. The width of all channels is 340 μm . (b) Time-dependent liquid displacement of the lattice networks with different D/Cs. (c) Liquid use efficiencies and elapsed times at 90% liquid displacement in the networks. The main network channel width varies $\sim 350 \mu\text{m}$ depending on the D/Cs geometries and is kept constant in each network. The numbers in the parentheses in (b) and (c) are the average D/C widths normalized by the main horizontal channel width. As the tapering ratio of D/Cs increases, both displacement time and liquid waste decrease

4. Conclusions

We have simulated liquid flow pattern in various channel geometries and identified the optimized networks allowing for more rapid and uniform liquid displacement with higher liquid use efficiency. The S-networks show high liquid use efficiency, but very slow displacement rate. When one takes into consideration the need for rapid displacement and low energy for the liquid injection, the H-networks are shown to be better candidates. Using the multiple-scale networks, such as the H-networks with wide and/or tapered D/Cs, improves both the liquid displacement rate and the liquid use efficiency, compared to the single-scale networks. Finally, we found that the lattice networks with the tapered D/Cs provide the most rapid and most visually uniform liquid displacement with minimal liquid loss. Representative simulation snapshots for all the network types included in this study can be found in Fig. S4 of Supplementary Information, which summarily illustrates the flow uniformity in each network type. Our final geometry tested here can be improved further by introducing additional features to improve the flow pattern in the network or widening and rounding the corners of the channels. Overall, these insights could complement the analytical and theoretical studies in the literature for the rapid and uniform flow and assist in the design of more cost effective smart window systems. Such improved networks could also be useful for other microfluidic functional materials, for instance, for self-healing materials, microreactors and energy harvesting devices where rapid delivery of reactive fluid to each point of compromised material integrity is critically important (Toohey, Sottos *et al.* 2007, Murphy and Wudl 2010, Hager, Greil *et al.* 2010, Koo and Velev 2013b, Liu, Li *et al.* 2010, Tondeur, Fan *et al.* 2011a, b, Renault, Colin *et al.* 2012).

Acknowledgments

The authors gratefully acknowledge the support from the NSF Triangle MRSEC for Programmable Soft Matter (DMR-1121107), the NSF-ASSIST Nanosystems Engineering Research Center (EEC-1160483), NSF award CBET 0828900 and Basic Science Research Program through the National Research Foundation of Korea (NRF) funded by the Ministry of Education (NRF-2015R1D1A1A01056812).

References

- Bejan, A. and Lorente, S. (2006), "Constructal theory of generation of configuration in nature and engineering", *J. Appl. Phys.*, **100**, 041301 1-27.
- Chang, S.T., Uçar, A.B., Swindlehurst, G.R., Bradley IV, R.O., Renk, F.J. and Velev, O.D. (2009), "Materials of controlled shape and stiffness with photocurable microfluidic endoskeleton", *Adv. Mater.*, **21**, 2803-2807.
- Cho, K.H. and Kim, M.H. (2010), "Fluid flow characteristics of vascularized channel networks", *Chem. Eng. Sci.*, **65**, 6270-6281.
- Commence, J.M., Saber, M. and Falk, L. (2011), "Methodology for multi-scale design of isothermal laminar flow networks", *Chem. Eng. J.*, **173**, 541-551.
- Domachuk, P., Tsioris, K., Omenetto, F.G. and Kaplan, D.L. (2010), "Bio-microfluidics: biomaterials and biomimetic designs", *Adv. Mater.*, **22**, 249-260.
- Gunther, A. and Jensen, K.F. (2006), "Multiphase microfluidics: from flow characteristics to chemical and

- materials synthesis”, *Lab Chip*, **6**, 1487-1503.
- Hager, M.D., Greil, P., Leyens, C., van der Zwaag, S. and Schubert, U.S. (2010), “Self-healing materials”, *Adv. Mater.*, **22**, 5424-5430.
- Hatton, B.D., Wheeldon, I., Hancock, M.J., Kolle, M., Aizenberg, J. and Ingber, D.E. (2013), “An artificial vasculature for adaptive thermal control of windows”, *Sol. Energ. Mat. Sol. C*, **117**, 429-436.
- Koo, H.J. and Velev, O.D. (2013a), “Ionic current devices—Recent progress in the merging of electronic, microfluidic, and biomimetic structures”, *Biomicrofluidics*, **7**, 031501 1-10.
- Koo, H.J. and Velev, O.D. (2013b), “Regenerable photovoltaic devices with a hydrogel-embedded microvascular network”, *Sci. Rep.*, **3**, 2357 (1-6).
- Lee, J., Lorente, S., Bejan, A. and Kim, M. (2009), “Vascular structures with flow uniformity and small resistance”, *Int. J. Heat Mass Tran.*, **52**, 1761-1768.
- Liu, H., Li, P.W. and Van Lew, J. (2010), “CFD study on flow distribution uniformity in fuel distributors having multiple structural bifurcations of flow channels”, *Int. J. Hydrogen Energ.*, **35**, 9186-9198.
- Mark, D., Haerberle, S., Roth, G., von Stetten, F. and Zengerle, R. (2010), “Microfluidic lab-on-a-chip platforms: requirements, characteristics and applications”, *Chem. Soc. Rev.*, **39**, 1153-1182.
- Morin, S.A., Shepherd, R.F., Kwok, S.W., Stokes, A.A., Nemiroski, A. and Whitesides, G.M. (2012), “Camouflage and display for soft machines”, *Science*, **337**, 828-832.
- Murphy, E.B. and Wudl, F. (2010), “The world of smart healable materials”, *Prog. Polym. Sci.*, **35**, 223-251.
- Olugebefola, S.C., Aragon, A.M., Hansen, C.J., Hamilton, A.R., Kozola, B.D., Wu, W., Geubelle, P.H., Lewis, J.A., Sottos, N.R. and White, S.R. (2010), “Polymer microvascular network composites”, *J. Compos. Mater.*, **44**, 2587-2603.
- Reis, A.H. (2006), “Constructal theory: from engineering to physics, and how flow systems develop shape and structure”, *Appl. Mech. Rev.*, **59**, 269-282.
- Renault, C., Colin, S., Orioux, S., Cognet, P. and Tzedakis, T. (2012), “Optimal design of multi-channel microreactor for uniform residence time distribution”, *Microsyst. Technol.*, **18**, 209-223.
- Russ, J.C. (2011), *The Image Processing Handbook*, sixth ed. Taylor & Francis Group, Boca Raton, FL, pp. 92-97.
- Saias, L., Autebert, J., Malaquin, L. and Viovy, J.L. (2011), “Design, modeling and characterization of microfluidic architectures for high flow rate, small footprint microfluidic systems”, *Lab Chip*, **11**, 822-832.
- So, J.H., Thelen, J., Qusba, A., Hayes, G.J., Lazzi, G. and Dickey, M.D. (2009), “Reversibly deformable and mechanically tunable fluidic antennas”, *Adv. Funct. Mater.*, **19**, 3632-3637.
- Solovitz, S.A. and Mainka, J. (2011), “Manifold design for micro-channel cooling with uniform flow distribution”, *J. Fluid Eng - T. ASME*, **133**, 0511103 1-11.
- Stone, H.A., Stroock, A.D. and Ajdari, A. (2004), “Engineering flows in small devices: microfluidics toward a lab-on-a-chip”, *Annu. Rev. Fluid Mech.*, **36**, 381-411.
- Tondeur, D., Fan, Y., Commenge, J.M. and Luo, L. (2011a), “Uniform flows in rectangular lattice networks”, *Chem. Eng. Sci.*, **66**, 5301-5312.
- Tondeur, D., Fan, Y. and Luo, L.G. (2011b), “Flow distribution and pressure drop in 2D meshed channel circuits”, *Chem. Eng. Sci.*, **66**, 15-26.
- Tondeur, D., Fan, Y., Commenge, J.M. and Luo, L. (2011c), “Flow and pressure distribution in linear discrete “ladder-type” fluidic circuits: an analytical approach”, *Chem. Eng. Sci.*, **66**, 2568-2586.
- Toohey, K.S., Sottos, N.R., Lewis, J.A., Moore, J.S. and White, S.R. (2007), “Self-healing materials with microvascular networks”, *Nat. Mater.*, **6**, 581-585.
- Uçar, A.B. and Velev, O.D. (2012), “Microfluidic elastomer composites with switchable vis-IR transmittance”, *Soft Matter*, **8**, 11232-11235.
- Wang, H., Iovenitti, P., Harvey, E. and Masood, S. (2002), “Optimizing layout of obstacles for enhanced mixing in microchannels”, *Smart Mater. Struct.*, **11**, 662-667.
- Wang, J. (2011), “Theory of flow distribution in manifolds”, *Chem. Eng. J.*, **168**, 1331-1345.
- Wang, K.M., Lorente, S. and Bejan, A. (2007), “Vascularization with grids of channels: multiple scales, loops and body shapes”, *J. Phys. D: Appl. Phys.*, **40**, 4740-4749.

Wu, W., Hansen, C.J., Aragon, A.M., Geubelle, P.H., White, S.R. and Lewis, J.A. (2009), "Direct-write assembly of biomimetic microvascular networks for efficient fluid transport", *Soft Matter*, **6**, 739-742.

CY

Supplementary Information

A. System parameters and constraints

The experimental conditions and fluid properties used in this simulation study were based on the experiment in our previous work (Uçar *et al.* 2012). We slightly modified some simulation parameters for simplicity in reading out the calculations. For instance, the original value of the fluid density of 61 wt. % glycerol-water mixture is 1156 kg m^{-3} and we rounded it down to 1000 kg m^{-3} in this study. We set 30 kPa as the starting pressure (outlet pressure is considered equal to zero), which is comparable to the pressure range used in the previous work. However, we used much lower inlet pressure (i.e., ΔP), 1 kPa, as the boundary condition for most of the simulations in this study to exhibit the clear advantage of H-networks over S-networks at lower inlet pressure. The detailed simulation conditions and parameters are listed in Table 1.

Table S1 Fluid properties, simulation parameters and constraints

Simulation Package and Model	COMSOL 4.2a Laminar Flow & Transport of Diluted Species	Diffusion Coefficient	$1 \times 10^{-10} \text{ m}^2 \text{ s}^{-1}$
Model Dimension	2D with shallow channel approximation	Density	1000 kg m^{-3}
Meshing	Physics-controlled (extremely fine)	Viscosity	0.01 Pa·s
Boundary Conditions	Constant ΔP and constant C	Matrix (Material) Area	864 (24×36) mm^2
Pressure Difference, ΔP (Inlet – Outlet)	1 kPa, (30 kPa in Fig.2(c))	Total Channel Area (Volume)	648 mm^2 (75% of the matrix area)
Inlet Concentration, C_{Inlet}	1 mol m^{-3}	Inlet & Outlet channel Dimensions (in 2D)	$1 \times 1 \text{ mm}$
Time Length, t	> 20 s	Channel Depth	0.3 mm
Constraints	Total matrix area, Total channel area (Volume)	Channel Width (Main Network)	0.35 – 0.95 mm

In most of our designs, Reynolds number (Re) at the inlet ranges from ~ 0.1 to ~ 10 , for both S- and H-networks, which indicates uniform laminar flow (Solovitz *et al.* 2011). Exceptions are the S-19 network with $\Delta P = 1 \text{ kPa}$ ($\text{Re} \ll 0.1$), and H-networks with $\Delta P = 30 \text{ kPa}$ ($\text{Re} \sim 30 - 100$).

We performed the simulations in 2D; however, the “Shallow Channel Approximation” was incorporated in the equations, which adds a drag term as a volume force to the fluid-flow equation, so that the frictional effect of the top and bottom channel walls on the flow is taken into account. A flow in a 2D model is only truly two dimensional if it is axisymmetric or the third dimension (thickness) is infinite. So if the material was thick enough, the effects of the side walls are negligible. However, this is not the case for the materials we experimented with, and this

approximation assumes the walls are close enough to account their effects on the flow.

Average Concentration values (mol m^{-3}) and Surface Concentration (mol m^{-1}) values were obtained directly from the functions of *Surface Average* and *Surface Integration* in COMSOL, respectively.

B. Data for liquid displacement in S- vs. H-shape networks

We compared H- and S-network designs with four different numbers of channels, i.e., 19, 25, 37, and 51. They all had the same inlet pressure of 1 kPa, but we also simulated same S-networks with increased inlet pressures of 30 kPa to analyze the effect of higher pressure drops. Figure S1 illustrates the average concentrations of the displacing liquid in all of the networks as a function of time. In all channel numbers, the H-networks clearly provide more rapid liquid replacement than the S-networks. For example, when the inlet pressure was kept constant at 1 kPa, none of the S-networks simulated in this study could reach 5% liquid displacement rate in 20 s (figure S1(b)), whereas the H-networks replace 30-80% of the liquid in the network at the same pressure and time (figure S1(a)). Even when the inlet pressure increases up to 30 kPa (figure S1(c)), the S-networks hardly achieve the liquid displacement percentages comparable to those of the H-networks within 20 s.

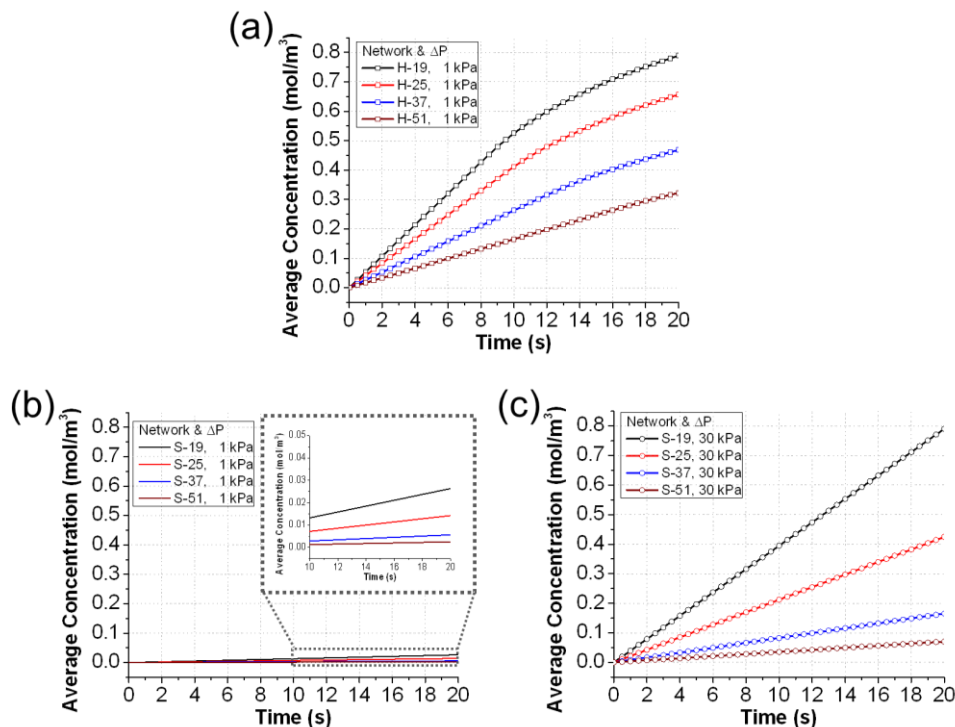


Figure S1 Time-dependent liquid displacement in (a) H-networks with varying channel numbers at 1 kPa inlet pressure, (b) S-networks with varying channel numbers at 1 kPa inlet pressure, (c) S-networks with varying channel numbers at 30 kPa inlet pressure. The H-networks provide more rapid liquid displacement than the S-networks even with 30 times less inlet pressures

C. H-51 networks with tapered and/or wide D/Cs

Introducing a second size-scale by tapering or widening the D/Cs drastically improves liquid displacement rate, flow uniformity, and liquid use in H-51 networks. The average concentrations of the displacing liquid in H-51 networks are plotted in figure S2 (the selected data set is shown in figure 4f). The wider or the more tapered (i.e., with higher tapering ratio) the D/Cs, the more rapid the liquid displacement speed (figure S2(c) and (d)). However, high tapering ratios have a disadvantage that they noticeably change the original rectangular shape of the network. To preserve the network close to the original rectangular shape, we modified top and bottom widths of the tapered D/Cs without changing the average D/C width. We designed a new network with the 5.5:2.5 tapered D/Cs (figure S2(a)), by widening the bottom part of the 7:1 tapered distributor channel and shortening its top edge, so in a sense D/Cs become both wide and tapered. Keeping the average D/C thickness same at the normalized width of “4”, a higher tapering ratio provides better flow uniformity, displacement rate and less liquid waste than any other ratio combinations, i.e., $7:1 > 5.5:2.5 > 4:4$ (figure 4d vs. S2a vs. 4b). Thus, this modification, i.e., widening and tapering D/Cs, provides an improved displacement performance than that of constant width D/C designs, but could not surpass the original tapered-only D/C performance (7:1).

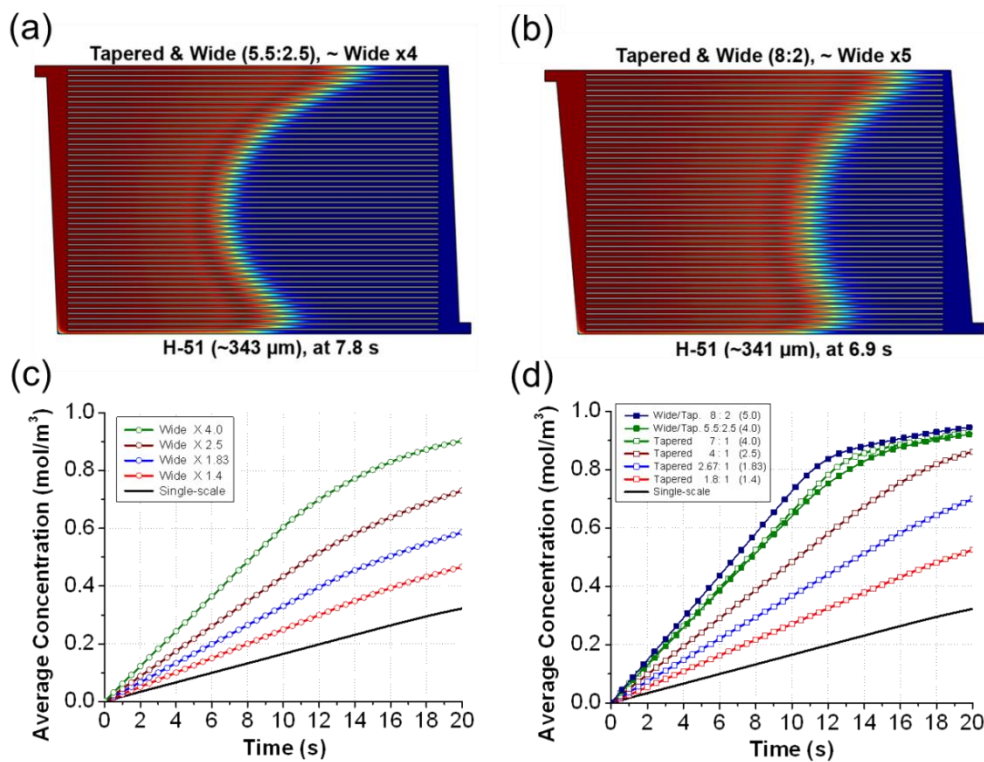


Figure S2 Simulation results of liquid displacement in the multiple-scale networks with the wide and the tapered D/Cs at the 50% liquid displacement; (a) D/Cs with the ratio of 5.5:2.5, (b) D/Cs with the ratio of 8:2. (c-d) Time-dependent average concentration in the H-51 networks with (c) the wide and (d) the tapered or the wide and tapered D/Cs. The wide D/Cs ratio reduces flow resistance of the network. Tapering the D/Cs improves the networks’ performance more significantly than simply using wide D/Cs, but it also creates a problem in the visual appearance of the channel networks

On the other hand, when we compare D/Cs with different average thicknesses, it is found that the primary effects of widening or tapering D/Cs is different: For example, comparing 7:1 (figure 4d, average thickness ratio is '4') vs. 8:2 (figure S2(b), average thickness ratio is '5'), we find that in terms of flow uniformity, the former, high tapering ratio, is superior because the flow in figure 4d has a more linear front line, and therefore less liquid will be wasted when it reaches to the outlet. However, the latter, less tapered but wider design results in more rapid liquid displacement compared to that of 7:1 (figure 4d). Interestingly both networks had the same amount of liquid waste rate, 2.1%, at the 50% liquid displacement. This comparison suggests that widening the D/Cs primarily improves the liquid displacement rate, and if the flow uniformity is the primary concern then D/Cs with high tapering ratios should be selected.

D. Liquid displacement in lattice networks with double tapering

Among the model networks presented so far, the lattice networks with tapered D/Cs provide the most rapid and visually uniform liquid displacement with minimal liquid loss. However, the addition of a third scale in the network could improve the network's performance even further. We incorporated the third different channel size by tapering the very top and bottom channels (T/Bs) in the main network (figure S3). In other words, all perimeter channels are tapered. The relative tapering ratios of top/bottom channels vs. left/right D/Cs were determined in accordance with the overall aspect ratio of the network's geometry. In a lattice network with double tapering in figure S3(b) (tapering ratios: D/Cs = 4:2 & T/Bs = 7:2), 90% of the liquid could be displaced in less than 10 s with a liquid waste rate of ~3.4% (see figure S3(d)). Displacing 99% of this network takes just ~13 s (figure S3(c)) where the liquid waste rate is only ~13%. The trend observed in the lattice networks with single tapering does not change in those with double tapering: as we increase the tapering ratio and/or the perimeter channel thickness, the flow rate and uniformity in the network increases as well. Although the lattice networks with single tapering preserves rectangular shape more than those with double tapering, the latter could achieve higher liquid displacement rate and liquid use efficiency, and more uniform flow (figure S4).

E. Characterization of flow uniformity of the simulated network geometries

Figure S4 provides an illustrative summary of the flow uniformity in each network type mentioned in this study. Although the S-network (figure S4(a)) has high liquid use efficiency, its displacement rate is very slow. The H-network (figure S4(b)) exhibits more rapid liquid displacement, even with its single-scale geometry. Using the multiple-scale, such as the H-networks with wide (figure S4(c)) and/or tapered (figure S4(d)) D/Cs, improves both the displacement rate and the liquid use efficiency compared to the single-scale networks. The performance of the lattice network (figure S4(e)) with tapering D/Cs surpasses that of the S- and H-networks. Our final geometry shown in figure 6 can be improved further by introducing additional features to the network. Figure S4(f) illustrates one of those improvement possibilities by tapering both D/C and T/B channels. By introducing a third scale in the network, the displacement rate becomes faster and more uniform flow is obtained.

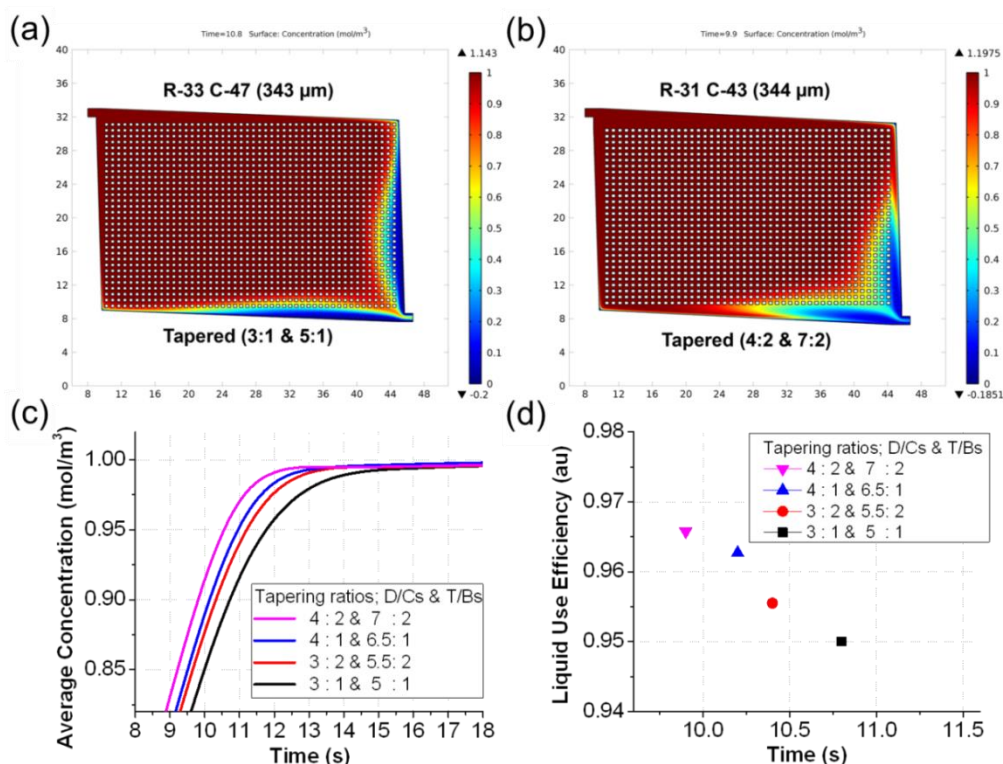


Figure S3 Performance of the lattice network with double tapering: Both D/Cs and T/Bs in the network are tapered. (a-b) Snapshots of the liquid flow patterns at the 90% liquid displacement in the modified lattice network with different tapering ratios; (a) 3:1 for D/C and 5:1 for T/B. (b) 4:2 for D/C and 7:2 for T/B. The numbers of the horizontal and the vertical channels (indicated as R and C in the labels, respectively) are different in a and b, due to the fixed area constraint. (c) Time dependent liquid displacement in the lattice networks with double tapering. (d) Liquid use efficiencies and the elapsed times in the lattice networks with double tapering at 90% liquid displacement. With double tapering, all the modified lattice networks tested displace 90% of the liquid in less than 11 s and waste less than 5% of the displacing liquid

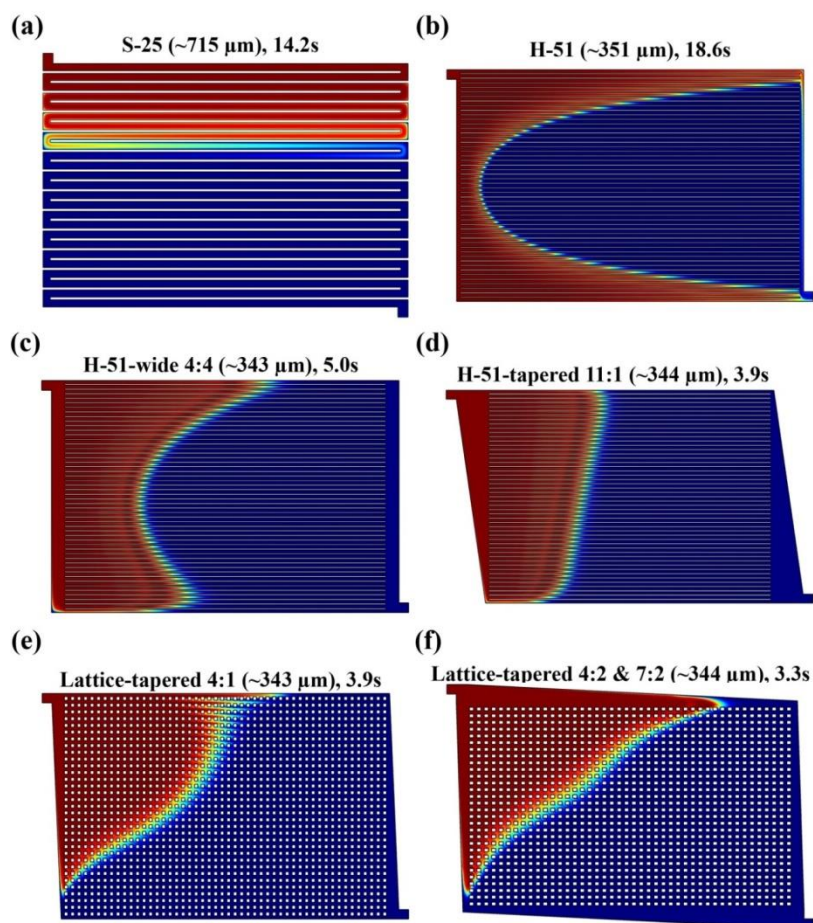


Figure S4 Comparison of various networks simulated in this study at the 30% liquid displacement, to illustrate flow uniformity performances of the networks: (a) Single-scale S-25 network with the inlet pressure of 30 kPa (the S-51 network could not displace 30% in the simulation times, thus we include here S-25 just to represent the flow uniformity of S-networks). (b) Single-scale H-51 network. (c) H-51 network with the 4 times wider D/Cs than those of the single-scale one in b. (d) H-51 network with the tapered D/Cs. The tapering ratio is 11:1. (e) Lattice network with the 4:1 tapered D/Cs. (f) Lattice network with double tapering (The tapering ratios: 4:2 for D/Cs & 7:2 for T/Bs). All the inlet pressures are 1 kPa, except S-25 in a, and channel sizes range from 343 μm to 351 μm